

Azobenzene Elastomers for Mechanically Tunable Diffraction Gratings

Shuying Bai and Yue Zhao*

Département de chimie, Université de Sherbrooke, Sherbrooke, Québec, Canada J1K 2R1, and Centre de recherche en science et ingénierie des macromolécules (CERSIM), Université Laval, Québec, Canada G1K 7P4

Received May 28, 2002; Revised Manuscript Received October 9, 2002

ABSTRACT: Three azobenzene-containing side-chain liquid crystalline polymers (SCLCPs) were grafted onto a styrene–butadiene–styrene (SBS) triblock copolymer to yield photoactive thermoplastic elastomers. The SCLCPs used were a polymethacrylate and two polyacrylates having different glass and phase transition temperatures. We have investigated the stretching-induced orientation of azobenzene mesogens, the orientation erasure by UV irradiation, and the consequences on the formation of diffraction gratings on stretched films. The results show that a combination of high degree of orientation of *trans*-azobenzene in nonirradiated areas with an efficient photoisomerization leading to disordered *cis*-azobenzene in irradiated areas is necessary for an efficient diffraction grating. However, this is not the only mechanism responsible for the formation of grating. Changes in the anisotropic morphology of stretched SBS may occur in these elastomers as a result of the photoisomerization process, which contributes to the formation of grating in films under strain and accounts for the stable diffraction grating remained in the relaxed state. These azobenzene elastomers can be used to record gratings that display reversible changes in diffraction angle and efficiency and the diffraction efficiency of which also depends strongly on the polarization of the probe light as well as the alignment of the fringes with respect to the strain of the film.

Introduction

Both azobenzene-containing amorphous and side-chain liquid crystalline polymers (SCLCPs) are attractive materials for holographic storage and photonic device applications.^{1–8} Studies on surface-relief gratings formed by movement of amorphous polymers on the surface^{9,10} and holographic gratings obtained from photochemical phase transition in SCLCPs³ illustrate the great interest generated by azobenzene polymers. Recently, we have shown that azobenzene elastomers may also be interesting to exploit.^{11,12} With elastomers, a new degree of freedom, namely, large and reversible deformation, can be used to assist the effects arising from photoisomerization for a control in the orientation of azobenzene groups. Using an easy preparation method,¹¹ an azobenzene SCLCP was grafted onto a styrene–butadiene–styrene (SBS) triblock copolymer, giving rise to an azobenzene thermoplastic elastomer. Orientation of azobenzene mesogens can easily be obtained by stretching a thin film at room temperature, and a subsequent exposure of the stretched film to UV and visible light erases and recovers the orientation as a result of the *trans*-to-*cis* and *cis*-to-*trans* photoisomerization, respectively. Moreover, it was found that irradiating a stretched film with UV light through a photomask resulted in a stable diffraction grating after the film was relaxed and that the grating could have its fringe spacing, diffraction angle, and diffraction efficiency changed reversibly upon elastic extension or retraction of the film.¹²

The study reported here aimed at revealing the role of the grafted azobenzene SCLCP in the orientation control and the formation of diffraction gratings. Three different SCLCPs were used, two of which are polyacrylates having different functional end groups on the azobenzene moiety and the other one is a polymethacry-

ate. As will be shown, the phase transition temperatures and photoisomerization behavior of azobenzene SCLCP determine largely the orientation of azobenzene mesogens induced by stretching, the orientation erasure upon UV irradiation, and the diffraction efficiency of gratings recorded on stretched films.

Experimental Section

The three azobenzene monomers used, denoted as M1, M2, and M3, were synthesized following the method described in the literature.¹³ Shown in Figure 1 are the chemical structures of the monomers and their corresponding SBS-based azobenzene elastomers, denoted as AE1, AE2, and AE3. For comparison, homopolymers were also prepared through radical polymerization of the monomers, yielding three azobenzene SCLCPs referred to as P1, P2, and P3 hereafter. For the synthesis of homopolymers, the typical reaction consisted in preparing a 5% monomer solution in toluene, in which was added 10 mol % of AIBN as initiator, with respect to the monomer mass. The homogeneous solution was then heated to 80 °C for 12 h of polymerization. Afterward, the polymer was purified by repeated precipitation in cold ether, collected, and dried in a vacuum oven. On the other hand, the three azobenzene elastomers were obtained using the method described in the previous paper,¹¹ with some minor modifications of conditions. A solution of SBS (Aldrich, 30% PS) in toluene was first prepared and heated to 80 °C (the concentration of SBS was around 15%), and then a 5% monomer/initiator solution in toluene was added into the hot SBS solution for 12 h of reaction; the initiator used was benzoyl peroxide, and its concentration was 5 mol %. As depicted in Figure 1, it is believed that the grafting of azobenzene SCLCP occurred mainly through radical transfer to the methylene group of the 1,4-polybutadiene (PB) block of SBS which initiates polymerization of the azobenzene monomer.^{11,15} Other possible reactions include copolymerization between the propagating polymer radicals and the double bonds of PB, which, however, is predominant only for 1,2-polybutadiene containing active vinyl groups.¹⁵ At this point, we could not confirm the suggested structure; the grafting sites could not be determined with certainty from ¹H NMR spectroscopy probably because of the small number of the azobenzene SCLCP grafts. Using a feed

* Corresponding author.

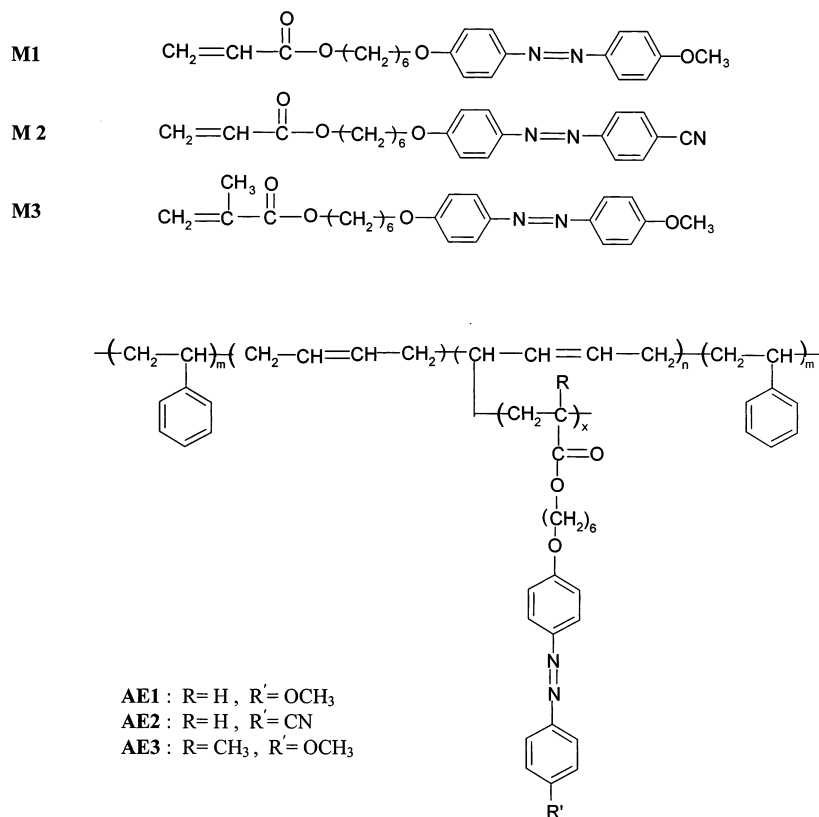


Figure 1. Chemical structure of monomers and azobenzene polymer-grafted SBS elastomers.

ratio of monomer/SBS around 1/1 for AE1 and AE3 and 2/1 for AE2, the three azobenzene elastomers obtained have a similar concentration of azobenzene SCLCP, close to 8%. The removal of homopolymers and unreacted monomers in the AE samples was ensured by multiple precipitations in methanol (for AE1 and AE2) or ethanol (for AE3) until the solution-cast films appear transparent and have a good mechanical strength like pure SBS. The films of AE samples also showed no birefringent domains on polarizing microscope, suggesting the formation of microdomains of the SCLCP grafts.¹¹ A couple of points should be mentioned here. First, AE1 is the elastomer investigated in the previous works,^{11,12} but a new sample was prepared and used in the present study. Second, we also tried to graft some other azobenzene polymers onto SBS using this method, but the attempts were unsuccessful. For instance, the reaction resulted in no grafting for a monomer having the same structure as M1 except the number of CH₂ units in the spacer (2 instead of 6). Characterizations of the samples were made by using differential scanning calorimetry (Perkin-Elmer DSC-7), polarizing microscopy (Leitz DMR-P), infrared spectroscopy (Bomem MB-200 FTIR), UV-vis spectroscopy (HP-8452A), ¹H NMR (Bruker AC-F 300), and gel permeation chromatography (GPC, Waters), using polystyrene standards and THF as eluent.

All films used for stretching and irradiation were prepared by casting a chloroform solution on the surface of a glass plate. They were dried at 50 °C in a vacuum oven for 2 days. For all irradiation experiments, the film thickness was carefully controlled to be about 10 μm under the initial strain. Irradiation with both a UV light (λ = 360 nm) and a visible light (λ = 440 nm) was performed using a 1000 W Hg (Xe) lamp (Oriol) and monochromatic filters. The actual intensities of UV and visible exposure were about 2 and 7 mW/cm². The orientation of azobenzene mesogens was monitored through polarized infrared spectroscopy, using the characteristic phenyl-oxygen stretching vibration band at 1254 cm⁻¹.¹⁴ More details were already reported.¹¹ To record diffraction gratings, a 30 min UV irradiation was applied with photomasks prepared from electron beam lithography. The mask was placed in front of the film, and a slight pressure was applied to ensure a good

Table 1. Characteristics of Homopolymers and Elastomers

polymer	azo content (wt %)	λ _{max} (nm)	T _g (°C)	M _w (g mol ⁻¹)	M _w /M _n
P1		358	46	5 800	1.2
P2		362	27	5 880	1.2
P3		358	68	64 200	2.7
AE1	7.7	359		215 700	2.0
AE2	8.6	363		177 000	2.0
AE3	8.1	359		168 100	2.1
SBS				174 500	1.4

contact between the film and the back of the masque. Using a He-Ne laser operating at 632.8 nm, the first-order diffraction efficiency (in the Raman-Nath regime) was measured as the ratio of the diffracted intensity (±1) over the intensity of the laser beam. (Higher values were obtained if the diffraction efficiency was calculated from the ratio of diffracted and transmitted intensities.) The photodiode was placed at a large distance (1 m) from the AE film to avoid scattering noise. In case the film was relaxed or stretched, the photodiode was displaced laterally to catch the diffracted signal, and its position was tuned by maximizing the measured intensity. Unless otherwise stated, diffraction gratings were inscribed with the fringes perpendicular to the strain and the polarization of the probe light was parallel to the strain.

Results and Discussion

Characterization of the Polymers. The characteristics of the synthesized azobenzene SCLCPs and their elastomers are presented in Table 1. All homopolymers have low molecular weights. As for elastomers, the grafting of SCLCP generally resulted in a slight increase in the average molecular weight and a wider distribution of molecular weights as compared to pure SBS. This can be seen from Figure 2 which compares the GPC curves of pure SBS and the three AE samples. All grafted samples display a broadened peak and a sig-

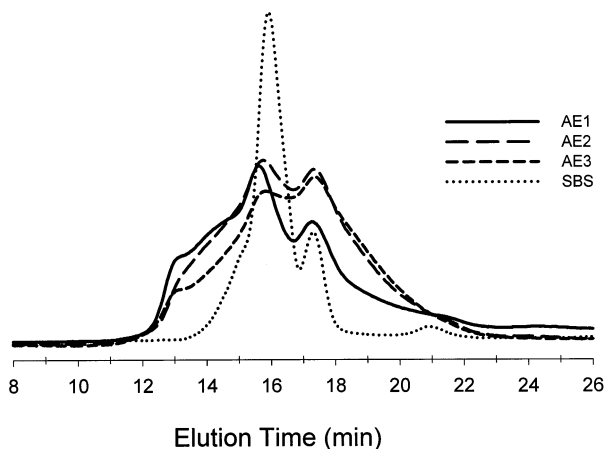


Figure 2. GPC curves of SBS and azobenzene polymer-grafted SBS elastomers.

nificant portion with lower elution times, which should correspond to SBS chains bearing grafted branches of azobenzene SCLCP since homopolymers can only have much longer elution times. However, there is also an increase in the portion with longer elution times, which may be indicative of some chain breaking during the reaction. This seems to be particularly possible at higher polymerization temperatures. Actually, some reactions were also carried out at 100 °C, and the resulting AE samples showed a decreased average molecular weight according to the GPC measurements. Also, Table 1 shows that AE3 has the lowest molecular weight among the azobenzene elastomers, while its corresponding homopolymere P3, obtained from the methacrylate monomer, has the highest molecular weight among the homopolymers. This result may be an indication of the competition between the grafting and homopolymerization reactions; that is, a more polymerizable monomer favors the formation of the homopolymere at the expense of its grafting onto the PB blocks. For the purpose of this study, the three AE samples used have a similar concentration of the azobenzene polymer, around 8%. A low concentration of azobenzene is better suited because the elastomer films are more transparent and mechanically stronger. The concentrations in Table 1 were determined from both UV-vis and ^1H NMR measurements, which yielded similar results. For UV-vis measurements, the azobenzene monomers and their corresponding elastomers were assumed to have the same extinction coefficients in chloroform solutions. As is seen in Table 1, the maximum absorption wavelengths of homopolymers and elastomers are almost identical in chloroform solutions.

None of the azobenzene homopolymers are miscible with SBS. Birefringent domains were observed on polarizing microscope for their blends. However, as already mentioned, no birefringent domains or liquid crystalline textures were observed for AE samples, suggesting that azobenzene SCLCP grafts be microphase-separated from SBS and dispersed in the PB matrix. Figure 3 shows the DSC heating curves (10 °C/min, second scan) of the homopolymers and elastomers. All homopolymers display two endotherms arising from the smectic-to-nematic and nematic-to-isotropic phase transitions (P2 has a narrow nematic range), and the polymethacrylate (P3) has a higher T_g than the two polyacrylates (P1 and P2). In the case of elastomers, the T_g for the azobenzene SCLCP grafts cannot be determined from the curves with certainty due to their small

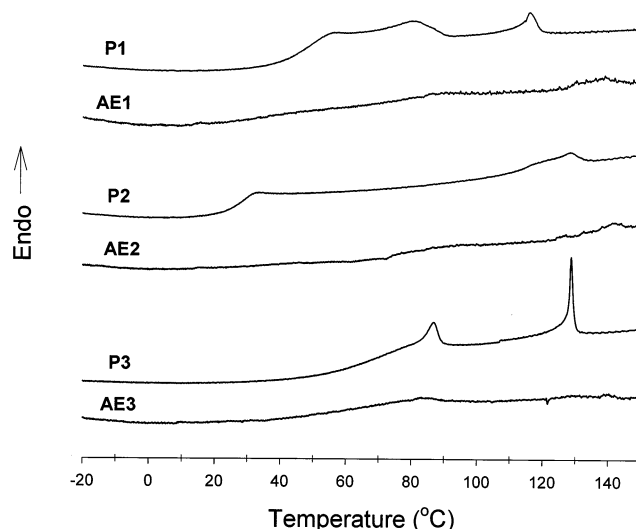


Figure 3. DSC heating curves of azobenzene homopolymers and elastomers.

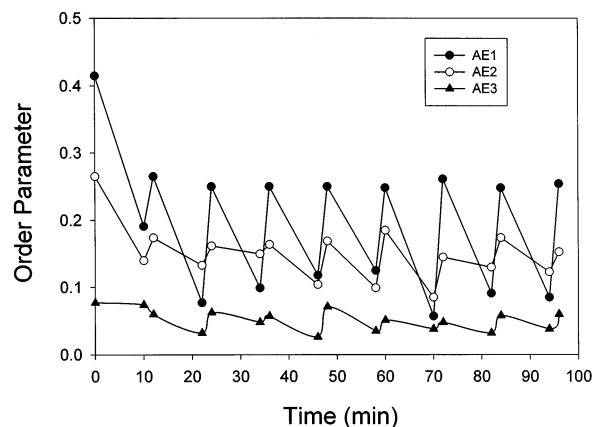


Figure 4. Changes in orientation of azobenzene mesogens in films of the three elastomers stretched at room temperature to draw ratio of 5 and subjected to repeated cycles of 10 min UV irradiation followed by 2 min visible irradiation.

concentrations, but their mesophases can be seen from the small endotherms on the curves. Interestingly, in all cases, the mesophase transitions seem to shift to higher temperatures in the elastomers as compared to the homopolymers, which may be revealing of some effects of the microdomains in the elastomers on the order of azobenzene mesogens and their phase transitions.

Orientation, Photoisomerization, and Diffraction Gratings. All AE films are colored but transparent. Like SBS films, they can be stretched and relaxed repeatedly at room temperature. For AE1, the previous study found that¹¹ stretching a film leads to orientation of *trans*-azobenzene mesogens along the strain direction, and this mechanically induced orientation can be erased by UV irradiation due to the *trans*-to-*cis* photoisomerization and recovered on visible irradiation due to the *cis*-to-*trans* back-isomerization. In the present study, this property was first investigated for the three elastomers. The plots of order parameter vs total irradiation time in Figure 4 are an example showing how the orientation of azobenzene mesogens in stretched films changes under repeated UV and visible irradiations. For each elastomer, the first data at zero time is the order parameter obtained after stretching a film at room temperature to a draw ratio of 5, i.e., 400% extension.

(The draw ratio is defined as the film length after stretching over that before stretching.) The film under strain was then exposed to 10 min unpolarized UV irradiation and 2 min unpolarized visible irradiation; following each irradiation the order parameter was measured. For each elastomer, the lower orientation level is observed after the UV irradiation, while the higher orientation level is established by the visible irradiation. Qualitatively, the switchable orientation is observed for the three elastomers, but significant differences are evident. Approximately, AE1 can have its orientation dropped to about 25% and recovered to 65% of the initial level on UV and visible irradiation, respectively. While for AE2, UV exposure can only decrease the orientation to about 50% of the initial value, and visible irradiation brings it back to 65%. As for AE3, the stretching-induced orientation is much lower than the two others, and the erasure and recovery seem to occur between 50% and 80% of the initial level. Varying parameters such as irradiation times, film thickness, and draw ratio change these values, but the trends remain the same. That is, a significant orientation of azobenzene mesogens can be induced by stretching films of AE1 and AE2 at room temperature, whereas the orientation degree is very low for AE3. Upon UV irradiation, the photoisomerization process converts more oriented *trans*-azobenzene to disordered *cis*-azobenzene in AE1 than in the two other elastomers.

Among the three elastomers, the very small orientation of AE3 may be explained by the relatively high T_g of this grafted azobenzene–polymethacrylate. Although its accurate value cannot be determined from the DSC measurement as mentioned above (Figure 3), judging from the T_g of the homopolymer, it should be in the range of 50 °C. The decrease in T_g of the elastomer as compared to the homopolymer arises from interfacial interactions between the azobenzene polymer and the PB matrix, which is elastic and has a low T_g of about –80 °C. Therefore, when AE3 films are stretched at room temperature, the microdomains of the azobenzene polymer are in the glassy state, and consequently, no effective orientation of azobenzene mesogens can be induced. The situation is different for the two azobenzene polyacrylates. Because of the lower T_g 's of the homopolymers, the T_g 's of the azobenzene grafts in AE1 and AE2 are likely to be below room temperature. Therefore, when stretched at ambient conditions, the azobenzene polymer is in a liquid crystalline phase, and a long-range orientation of the azobenzene mesogens can readily be developed. However, on UV irradiation, the orientation erasure in AE1 is significantly greater than in AE2. This difference may be explained by their different photoisomerization behaviors.

Figure 5 presents the UV–vis spectra taken from unstretched thin films of the three elastomers before irradiation (thick lines) and after 10 min irradiation (thin lines). In all cases, the *trans*-to-*cis* photoisomerization occurs during the exposure, leading to a decrease in absorbance of the broad peaks around 360 nm for *trans*-azobenzene, while the increase in population of *cis*-azobenzene is seen from the peaks around 450 nm. As pointed out above, this process is at the origin of the orientation erasure on UV irradiation. However, as compared with AE1 and AE3, the spectral changes of AE2 are clearly less important. Figure 6 shows the changes in absorbance of the peak of *trans*-azobenzene, normalized with the absorbance before irradiation,

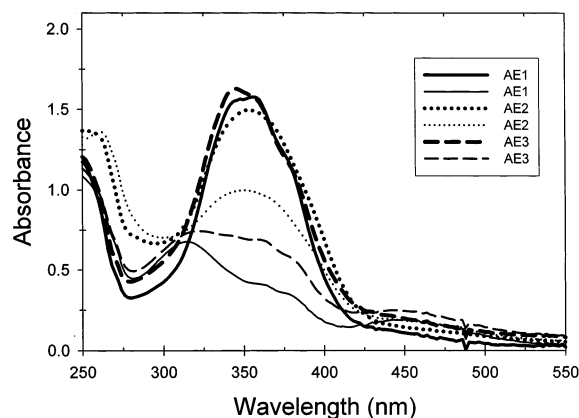


Figure 5. UV–vis spectra of unstretched films of the three elastomers before irradiation (thick lines) and after 10 min UV irradiation (thin lines).

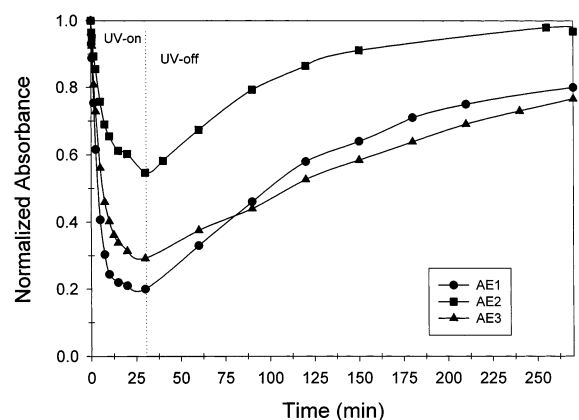


Figure 6. Changes in normalized absorbance of *trans*-azobenzene for unstretched films of the three elastomers as a function of time during a 30 min UV irradiation followed by a 4 h period with irradiation turned off.

during a 30 min period of UV irradiation and a subsequent 4 h period after turning off the irradiation. For AE2, not only is the reduction in population of *trans*-azobenzene upon UV irradiation much slower than AE1 and AE3, its thermally induced *cis*-to-*trans* backisomerization is much faster. These results suggest that under continuous UV irradiation the equilibrated population of *cis*-azobenzene in AE2 is smaller than in AE1 and AE3, which accounts for the limited decrease in orientation of azobenzene mesogens. Both AE1 and AE3 have an OCH₃ end group in their azobenzene moiety while AE2 carries a CN group in its azobenzene moiety, which results in a shorter lifetime for the *cis* isomer.

Diffraction gratings can be recorded on stretched films of the three elastomers by UV irradiation through a photomask. A priori, the periodic modulation of the refractive index should mainly arise from disordered *cis*-azobenzene in exposed areas and oriented *trans*-azobenzene in nonirradiated areas. As will be argued later, the differences in azobenzene orientation and conformation are not the only mechanism responsible for the formation of grating. After recording, as the stretched film is highly anisotropic, when viewed on polarizing microscope, no grating can be seen if the strain direction is parallel to one of the crossed polarizers. However, rotating the film by a small angle reveals the grating with irradiated areas appearing much darker than nonirradiated areas. Using a phase-contrast microscope, the grating is clearly observable whatever the position

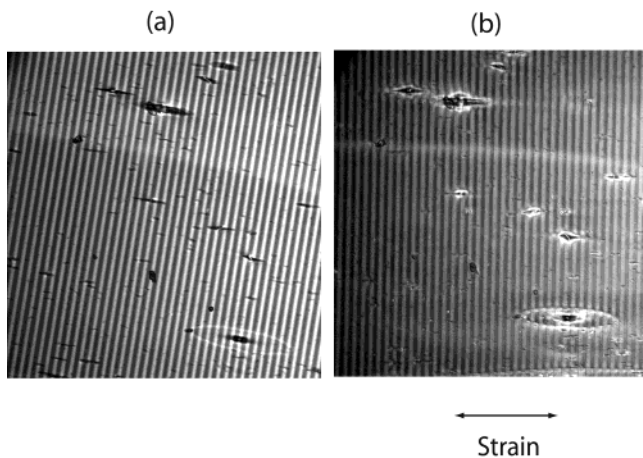


Figure 7. Optical micrographs of a grating recorded on an AE1 film stretched to draw ratio of 5: (a) viewed on polarizing microscope by placing the strain direction at 5° to crossed polarizers; (b) viewed on a phase-contrast microscope. The strain direction is normal to the fringes. The fringe spacing of the grating is $10 \mu\text{m}$.

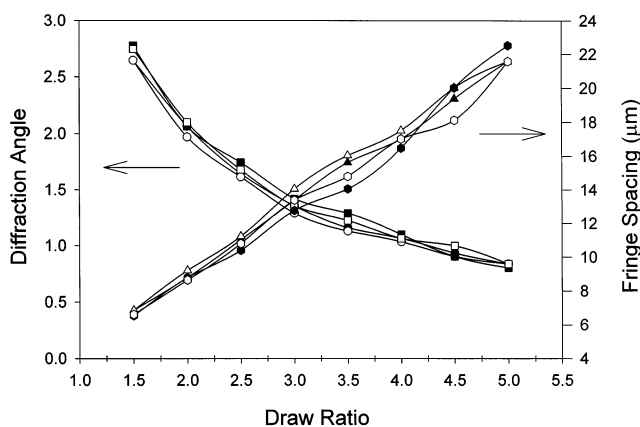


Figure 8. First-order diffraction angle and fringe spacing vs draw ratio for a grating inscribed on an AE2 film stretched to draw ratio of 5 and subjected to two cycles of retraction (closed symbols) and extension (open symbols).

of the stretched film. Figure 7 shows an example of a same grating of $10 \mu\text{m}$ fringes, recorded on an AE1 film stretched to a draw ratio of 5, viewed on both a polarizing microscope, by rotating the strain direction by about 5° to crossed polarizers, and a phase-contrast microscope, without rotation of the film. A number of elongated defects can be seen on the surface of the film as they were amplified by the large deformation of the elastomer. When a stretched film with a grating is repeatedly relaxed and stretched, diffraction angles increase or decrease as a result of reversible changes in the period of the grating. From the measured first-order diffraction angle Θ , the fringe spacing can be calculated from $\Lambda = \lambda / (2 \sin \Theta)$, where λ is the wavelength of the He-Ne laser. An example of results is given in Figure 8 for an AE2 film initially stretched to a draw ratio of 5 for the recording of a grating and then subjected to two cycles of relaxation and extension of the film. Both the diffraction angle and fringe spacing change reversibly within experimental errors. The period of grating was simply linearly proportional to the film deformation.

The first-order diffraction efficiency was also measured as a function of draw ratio. Figure 9 shows some results obtained for the three elastomers under the

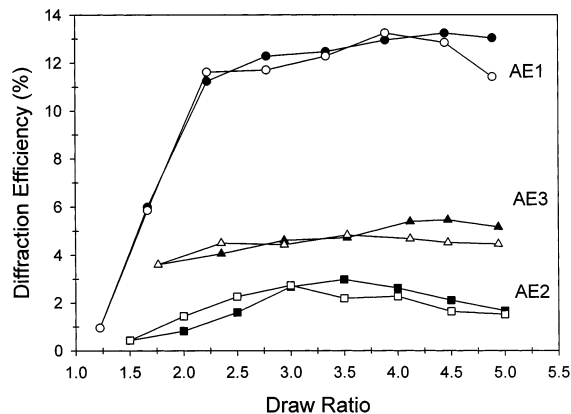


Figure 9. First-order diffraction efficiency vs draw ratio for gratings inscribed on films of the three elastomers stretched to draw ratio of 5 and subjected to retraction (closed symbols) and extension (open symbols). The measurements were performed immediately after recording of the gratings.

same conditions. In this experiment, the film of each elastomer was first stretched to a draw ratio of 5 at room temperature and then exposed to UV irradiation through a photomask of $20 \mu\text{m}$ fringe spacing. Immediately following the recording of grating, the diffraction efficiency was measured while relaxing and stretching the film for two cycles. For the sake of clarity, only data for the first cycle of deformation are presented; the second cycle gave rise to the same results. The three elastomers behave differently, among which AE1 shows the highest diffraction efficiency ($\sim 13\%$). In all cases, however, changes in diffraction efficiency on retraction and extension of the film are reversible within experimental errors. For AE1, the diffraction efficiency remains essentially unchanged over a wide range of large deformations despite the change in the period of grating. It then drops quickly when the draw ratio is under 2. For AE2, the diffraction efficiency is much lower than AE1 and strongly dependent on the deformation, going through a maximum of about 3% at a draw ratio around 3. In contrast with AE1 and AE2, the diffraction efficiency of AE3 varies little with the deformation, ranging from near 5% to 3% in the relaxed film. A number of factors may contribute to determine the diffraction efficiency. Nevertheless, as explained above, the gratings here should be mainly volume gratings arising from periodic changes in orientation and conformation of the azobenzene mesogens. In nonirradiated areas the orientation of *trans*-azobenzene is that induced by stretching, but this orientation decreases in irradiated areas due to the appearance of disordered *cis*-azobenzene. As is shown in Figure 4, among the three elastomers AE1 has the highest orientation induced by stretching and the largest decrease in orientation on UV irradiation, which means the largest change in refractive index and which explains the highest diffraction efficiency observed. The almost constant diffraction efficiency at large deformations may be explained by the fact that the stretching-induced orientation in nonirradiated areas is similar for draw ratios above 2, which is characteristic of SCLCPs.¹⁶ When the film is completely relaxed, the orientation is lost, and the difference in refractive index is mainly between disordered *trans*-azobenzene in nonirradiated areas and *cis*-azobenzene in irradiated areas. This difference must be very small because the elastomer contains only about 8% of the azobenzene SCLCP, which results in the rapid decrease

in diffraction efficiency as the film is approaching the relaxed state. In line with the above discussion, lower diffraction efficiency would be expected for AE2 and AE3. In the case of AE2, the orientation erasure on UV irradiation is limited, while for AE3, its stretching induced orientation is already very small. Qualitatively, the results in Figure 9 are consistent with the analysis. However, a closer look at the results suggests that changes in orientation of azobenzene mesogens should not be the sole factor determining the diffraction. In the case of AE3, there is little orientation in the stretched film even before irradiation so that a periodic change in orientation after irradiation should not be the primary factor for the diffraction grating. This actually is reflected by the absence of a rapid drop in diffraction efficiency for AE3 in the relaxed state. The diffraction efficiency of AE3 is much lower than AE1 but greater than AE2, which cannot be accounted for only by differences between *trans*-azobenzene and *cis*-azobenzene of the 8% azobenzene polymer. In other words, some structural or morphological rearrangements of SBS related to photoisomerization of azobenzene mesogens in irradiated areas may take place. This hypothesis was indeed supported by a number of experiments, some of which are discussed below.

On one hand, note that the measurements described in Figure 9 were completed within about 1 h after the UV irradiation for recording of the grating. Because of the very slow thermally induced *cis*-to-*trans* back-isomerization in the films (Figure 6), most *cis*-azobenzene remained in irradiated areas during the experiments. After the measurements, the relaxed films were kept in the dark. It was found that the thermal back-isomerization was completed after about 4 h for AE2 and 10 h for AE1 and AE3. So once the equilibrated *trans*-rich state was recovered in the relaxed films after 10 h, in principle, any remaining grating due to the periodic presence of *trans*-azobenzene and *cis*-azobenzene should disappear. A restretching of those films should result in no grating because the stretching induces orientation of *trans*-azobenzene throughout the whole film. However, when the three relaxed films were examined 2 weeks later, gratings were still observable by the microscope, although less prominent than those shortly after UV irradiation. These stable gratings should be the result of some permanent structural rearrangement in the elastomers, which was induced by the photoisomerization process. Their first-order diffraction efficiencies were measured again during tow cycles of stretching and retraction, and data of the first cycle are presented in Figure 10. The results show that in all cases the diffraction efficiency is significantly reduced but still varies reversibly with deformation. Interestingly, the remaining grating of AE3 has the least decrease in diffraction efficiency among the elastomers, which implies that its grating formed during UV irradiation would indeed be due to a structural rearrangement rather than changes in orientation of azobenzene mesogens, as discussed above.

On the other hand, it was found that the diffraction efficiency is strongly dependent on the polarization of the probe light as well as the alignment of the fringes with respect to the strain direction. For all the experiments discussed above, gratings were recorded with the fringes perpendicular to the strain, and the diffraction efficiency was measured with the polarization of light parallel to the strain, for which the diffraction is at the

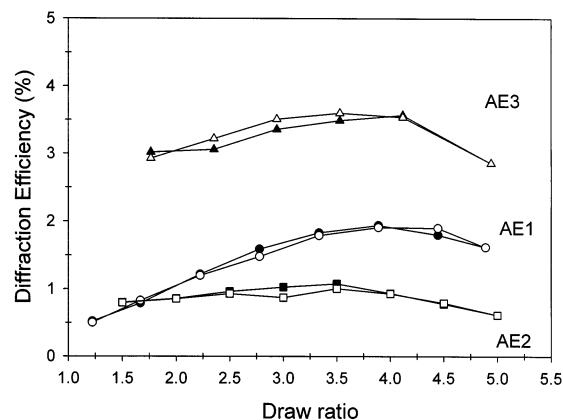


Figure 10. First-order diffraction efficiency vs draw ratio for gratings remained in the same films as in Figure 9, 2 weeks after the recording of gratings. The films were subjected to stretching (closed symbols) and retraction (open symbols).

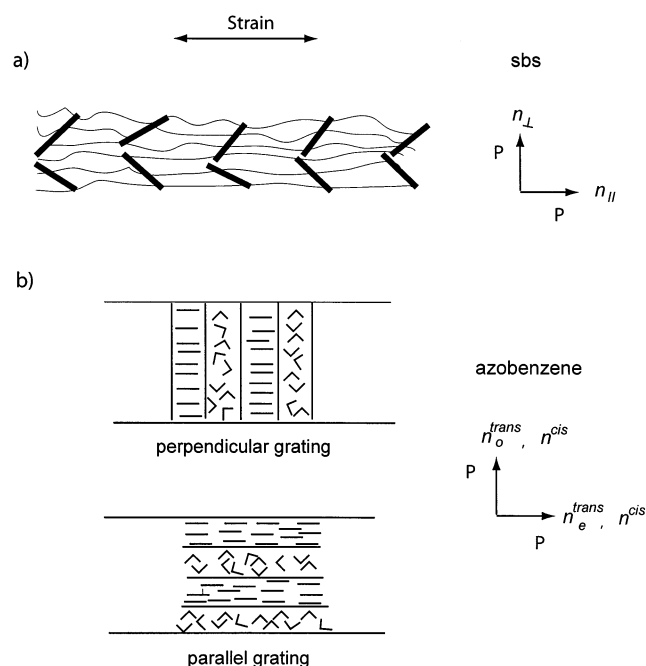


Figure 11. Schematic illustration of (a) the anisotropic morphology of stretched SBS and (b) the periodic presence of disordered *cis*-azobenzene and oriented *trans*-azobenzene in irradiated and nonirradiated fringes, respectively, for both perpendicular and parallel gratings.

maximum. The diffraction efficiency decreases as the polarization makes an angle to the strain and reaches the lowest value when the polarization is normal to the strain direction, as already reported in the previous communication.¹² More drastic effects on the diffraction were observed from the alignment of the fringes relative to the strain direction. When the fringes were inscribed parallel to the strain (parallel grating), a considerable decrease in diffraction was found for all the elastomers. For AE1, under the same conditions of recording, the diffraction efficiency of a parallel grating was dropped to below 50% of that of a perpendicular grating. For AE2 and AE3, in most cases the diffraction of parallel gratings was so weak that it could not be measured with certainty. This feature also hints for a structural rearrangement in the elastomers, as can be argued in a simplistic way using the schematic illustration in Figure 11.

It is known that in a highly stretched SBS film oriented PB chains are supported by PS cylindrical microdomains inclined to the strain and that rearrangement of PS cylinders can occur even at $T < T_g$ of the PS microdomains, being accompanied by changes in orientation of the rubbery PB chains.^{17,18} For the azobenzene elastomers, it is well conceivable that photoisomerization of azobenzene mesogens, which are dispersed in the PB matrix, could affect oriented PB chains and results in rearrangement of PS cylinders. Considering the SBS as a background, the probe light sees different refractive indices, n_{\parallel} and n_{\perp} , with its polarization parallel or perpendicular to the strain. As for the azobenzene polymer, in both parallel and perpendicular gratings depicted in Figure 11, irradiated areas mainly contain disordered, bent-shaped *cis*-azobenzene and nonirradiated areas contain oriented, rodlike *trans*-azobenzene. For a given polarization of light, the diffraction efficiency of both parallel and perpendicular gratings should be similar if (1) the SBS background undergoes no changes initiated by photoisomerization of azobenzene in irradiated areas or (2) same changes in SBS occur in irradiated areas regardless of the alignment of the fringes. Because under those conditions, the differences in refractive index between irradiated and nonirradiated areas should mainly arise from differences between disordered *cis*-azobenzene and oriented *trans*-azobenzene. As already mentioned, this is not the case. The perpendicular grating shows much higher diffraction efficiency than the parallel grating. Because of the highly anisotropic morphology of stretched SBS, it is possible that structural rearrangement of SBS associated with photoisomerization of azobenzene be more severe in perpendicular gratings than in parallel gratings.¹⁹ Another interesting observation that can be made from Figure 11 is about the contribution of azobenzene mesogens to the observed strong polarization dependence of the diffraction efficiency. In both cases of parallel and perpendicular fringes, when the polarization of light is parallel to the strain, light sees the extraordinary refractive index of *trans*-azobenzene, n_e^{trans} , in nonirradiated areas and the average refractive index of *cis*-azobenzene, n^{cis} , in irradiated areas. In the case where the polarization of light is perpendicular to the strain, light senses the ordinary refractive index of *trans*-azobenzene, n_0^{trans} , in nonirradiated areas and still n^{cis} in irradiated areas. In the latter case, the diffraction efficiency is smaller because the difference between n_0^{trans} and n^{cis} is smaller than the difference between n_e^{trans} and n^{cis} .

Conclusion

Three azobenzene elastomers were prepared by grafting different azobenzene SCLCPs onto SBS. The orientation of azobenzene mesogens in films stretched at room temperature is governed by T_g of the SCLCP. Orientation can effectively be induced if the azobenzene grafts in the elastomer are in a liquid crystalline phase at ambient conditions. Erasure of the orientation in stretched films by UV irradiation is determined by the equilibrated concentration of *cis*-azobenzene resulting from the *trans*-to-*cis* photoisomerization. These azobenzene elastomers can be used to record mechanically tunable diffraction gratings that display reversible changes in diffraction angle and efficiency upon elastic extension and relaxation of the film. Two interesting situations were observed. First, if stretching leads to high orientation of azobenzene mesogens and UV ir-

radiation results in an efficient erasure of the orientation in the stretched film, which is the case for AE1, the grating formed, showing the highest diffraction efficiency among the elastomers is mainly an orientation grating between oriented *trans*-azobenzene in nonirradiated areas and disordered *cis*-azobenzene in irradiated areas. In this case, the diffraction efficiency may be almost constant at large deformations of the film as long as the orientation of *trans*-azobenzene remains; however, it becomes very sensitive to small deformations as the orientation of azobenzene is lost in the relaxed state. Second, even when stretching results in little orientation of azobenzene mesogens in the film, which is the case for AE3, grating with significant diffraction efficiency can still be formed possibly through some morphological changes in stretched SBS involving PB orientation and rearrangement of PS cylinders, which are initiated by the photoisomerization process of azobenzene in irradiated areas. In this case, the diffraction efficiency varies relatively little with deformation of the film and shows no abrupt drop in the relaxed state. Whatever the dominant contribution to the formation of the diffraction grating on the stretched film, the structural and morphological changes in SBS should be responsible for the stable gratings observed in the relaxed state for all the elastomers, because any differences in both orientation and conformation of azobenzene in irradiated and nonirradiated areas should disappear in the relaxed state after about 10 h, with the completion of the thermal *cis*-to-*trans* back-isomerization. Moreover, gratings on stretched films of azobenzene elastomers display a strong dependence of the diffraction efficiency on the polarization of the probe light as well as the alignment of the fringes with respect to the strain. Part of the explanation may come from changes in SBS, which would be different according to the alignment of the fringes as stretched SBS has a highly anisotropic morphology. More studies are underway in order to understand the stable grating related to structural rearrangement occurred in these elastomers.

Acknowledgment. Financial support from the Natural Sciences and Engineering Research Council of Canada and the Fonds pour la Formation de Chercheurs et l'Aide à la Recherche de Québec is acknowledged.

References and Notes

- (1) Ichimura, K. *Chem. Rev.* **2000**, *100*, 1847.
- (2) Eich, M.; Wendorff, J. H. *Makromol. Chem. Rapid Commun.* **1987**, *8*, 59.
- (3) (a) Ikeda, T.; Tsutsumi, O. *Science* **1995**, *268*, 1873. (b) W. Y.; Zhang, Q.; Kanazawa, A.; Shiono, T.; Ikeda, T.; Nagase, Y. *Macromolecules* **1999**, *32*, 3951. (c) Yamamoto, T.; Hasegawa, M.; Kanazawa, A.; Shiono, T.; Ikeda, T. *J. Mater. Chem.* **2000**, *10*, 337.
- (4) (a) Fischer, T.; Lasker, L.; Rutloh, M.; Czaplá, S.; Stumpe, J. *Mol. Cryst. Liq. Cryst.* **1997**, *299*, 293. (b) Fischer, T.; Lasker, L.; Stumpe, J.; Kostromin, S. *J. Photochem. Photobiol. A: Chem.* **1994**, *80*, 453.
- (5) Hvilsted, S.; Andruzzi, F.; Fulinna, C.; Siesler, H. W.; Ramanujam, P. S. *Macromolecules* **1995**, *28*, 2172.
- (6) (a) Natansohn, A.; Rochon, P.; Gosselin, J.; Xie, S. *Macromolecules* **1992**, *25*, 2268. (b) Rochon, P.; Batalla, E.; Natansohn, A. *Appl. Phys. Lett.* **1995**, *66*, 136.
- (7) (a) Kim, D. Y.; Li, L.; Jiang, X. L.; Shivshankar, V.; Kumar, J.; Tripathy, S. K. *Macromolecules* **1995**, *28*, 8835. (b) Viswanathan, N.; Kim, D. Y.; Bian, S.; Williams, J.; Liu, W.; Li, L.; Samuelson, L.; Kumar, J.; Tripathy, S. K. *J. Mater. Chem.* **1999**, *9*, 1941.

- (8) (a) Laurence, C.; Zhao, Y. *Macromolecules* **1999**, *32*, 3195.
(b) Zhao, Y.; Chenard, Y.; Paiement, N. *Macromolecules* **2000**, *33*, 1049. (c) Zhao, Y.; Chenard, Y.; Galstian, T. *Appl. Phys. Lett.* **2000**, *77*, 2644.
- (9) Rochon, P.; Batalla, E.; Natansohn, A. *Appl. Phys. Lett.* **1995**, *66*, 136.
- (10) Kim, D. Y.; Tripathy, S. K.; Li, L.; Kumar, J. *Appl. Phys. Lett.* **1995**, *66*, 1166.
- (11) Bai, S.; Zhao, Y. *Macromolecules* **2001**, *34*, 9032.
- (12) Zhao, Y.; Bai, S.; Dumont, D.; Galstian, T. *Adv. Mater.* **2002**, *14*, 512.
- (13) Ringsdorf, H.; Schmidt, H.-W. *Makromol. Chem.* **1984**, *185*, 1327.
- (14) Nair, B. R.; Gregoriou, V. G.; Hammond, P. T. *Polymer* **2000**, *41*, 2961.
- (15) Odian, G. *Principles of Polymerization*, 3rd ed.; John Wiley & Sons: New York, 1991.
- (16) Zhao, Y.; Lei, H. *Polymer* **1994**, *35*, 1419.
- (17) Pakula, T.; Saijo, K.; Kawai, H.; Hashimoto, T. *Macromolecules* **1985**, *18*, 41294.
- (18) Zhao, Y. *Macromolecules* **1992**, *25*, 4705.
- (19) According to our preliminary studies on the kinetics for the formation of grating using holographic recording, in addition to the azobenzene grating formed at the beginning of the exposure, a second grating develops at longer times, which is revealing of structural rearrangements occurring inside the stretched film. The nature of these changes is under investigation.

MA020822B